On the drivers of regime shifts in the Antarctic marginal seas

Verena Haid[1], Ralph Timmermann[1], Özgür Gürses[1], and Hartmut H. Hellmer[1]

[1]Alfred Wegener Institute Helmholtz Centre for Polar and Marine Research, Bremerhaven, Germany

Correspondence: Verena Haid (verena.haid@awi.de)

Abstract. Recent studies found evidence for a potential future tipping point when the density of Antarctic continental shelf waters, specifically in the southern Weddell Sea, allows the onshore flow of warm waters of open ocean origin. A cold-to-warm shift in the adjacent ice shelf cavities entails a multiplication of ice shelf basal melt rates and can possibly trigger instabilities in the ice sheet. From a suite of numerical experiments, aimed to force such a regime shift on the continental shelf, we identified

5   the density balance between the shelf waters formed by sea ice production and the warmer water at the shelf break as the deciding element for a tipping into a warm state. In our experiments, this process is reversible but with evidence for hysteresis behaviour. Using HadCM3 20th-century output as atmospheric forcing, the resulting state of the Filchner-Ronne cavity depends on the initial state. In contrast, ERA Interim forcing pushes even a warm initialisation into a cold state, i.e., the system back to the cold side of the reversal threshold. However, it turns out that for forcing data perturbations of a realistic magnitude, a unique

10   and universal recipe for triggering a regime shift in Antarctic marginal seas does not exist. Whether or not any given forcing or perturbation yields a density imbalance and thus allows for the inflow of warm water depends on the interplay between bottom topography, mean ocean state, sea ice processes, and atmospheric conditions.

1 Introduction

In the context of climate change, the accurate prediction of future climate evolution for different scenarios and the identification

15   of crucial thresholds depends on a realistic representation of tipping points in the relevant climate components. For the polar environment, these components are the atmosphere, ocean, and cryosphere. A tipping point can trigger an accelerated regime shift that, without thorough knowledge of the interplay of the components involved, cannot be predicted from observations of current trends. Crossing a tipping point not only causes rapid and hard-to-predict changes after the triggering component has crossed an invisible threshold, but these changes also cannot be reversed simply by a return of said triggering components to

20   the other side of the threshold (Lenton et al., 2008; Klose et al., 2020). Typically, a reversal is either impossible or necessitates a return of the forcing components far beyond the tipping point threshold towards a 'reversal threshold'. In between these two thresholds an area of bi-stability exists, where the state of the climate depends on its own previous state (Fig. 1).

One of the possible regime shifts in polar climate is the change of the Antarctic continental shelf from a cold to a warm state. Supported by atmospheric forcing, bottom topography, and/or cavity shelf-sea interaction (Thoma et al., 2008; Nakayama

25   et al., 2013; Jourdain et al., 2017), the warming can migrate beneath fringing ice shelves (Jenkins et al., 2010) enhancing basal melting and causing instabilities of both the grounding line and the ice-shelf-feeding ice sheet (Gladstone et al., 2012;
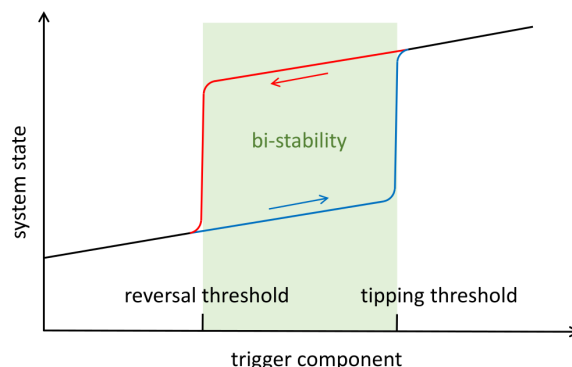
Figure 1. Schematic depiction of tipping hysteresis behaviour.

Cornford et al., 2015). For the Filchner-Ronne Ice Shelf (FRIS) in the southern Weddell Sea, such a change has been found in simulations using future climate scenarios (Hellmer et al., 2012; Naughten et al., 2021), and observations seem to support the possibility of such an event in the future (Darelius et al., 2016; Ryan et al., 2020). Timmermann and Hellmer (2013) suggest

30 that the decrease in sea ice production and concurrent freshening of shelf waters trigger the regime shift, which according to Hellmer et al. (2017) is irreversible as long as the meltwater input is high. In addition, Hattermann et al. (2021) emphasize the key role of off-shore winds in controlling sea ice formation, shelf water densification, and sub-ice shelf circulation.

Several regional models indicate further drivers of a regime shift in the southern Weddell Sea. Daae et al. (2020) identify two necessary conditions for the flow of warm water of open ocean origin into the FRIS cavity: (a) freshening of shelf waters and

35 (b) relaxation of the Antarctic Slope Front (ASF) density gradient, which was imposed by lifting the thermocline by several hundreds of meters. Naughten et al. (2019) suggest a connection between position and intensity of the Weddell polynya and the transport of Warm Deep Water (WDW) onto the southern continental shelf caused by density changes at the shelf break. The onshore flow, saltier and thus denser, enhances the sub-ice shelf circulation and melting at the FRIS base. The impact of the polynya is visible until roughly 14 years after cessation of the polynya's deep convection. In an perturbation experiment, Bull

40 et al. (2021) indicate that water mass properties of the slope current in the eastern Weddell Sea have an impact on the onshore flow of warmer waters and thus on FRIS basal melting. The recovery of the cold state after a regime shift takes 5—15 years depending on the slope current characteristics and the strength of perturbation. The findings agree with earlier model results suggesting that sea ice and surface water anomalies near the Greenwich meridian have a strong impact on bottom salinity on the southern and western Weddell Sea continental shelf (Hellmer et al., 2009). In an idealized setting, Hazel and Stewart (2020)

45 present a conceptual model in which the FRIS cavity state is determined by the water masses, either High Salinity Shelf Water (HSSW) or WDW, flooding the cavity. Plotting the cavity state against the controlling variable (meridional winds), they obtain a hysteresis with bi-stabilities (cf. Fig. 1).

The EU Horizon 2020 project 'Tipping Points in Antarctic Climate Components (TiPACCs)' addresses possible near-future tipping points in the Southern Ocean and the Antarctic Ice Sheet. Within this project, we investigated the possible cold-to-
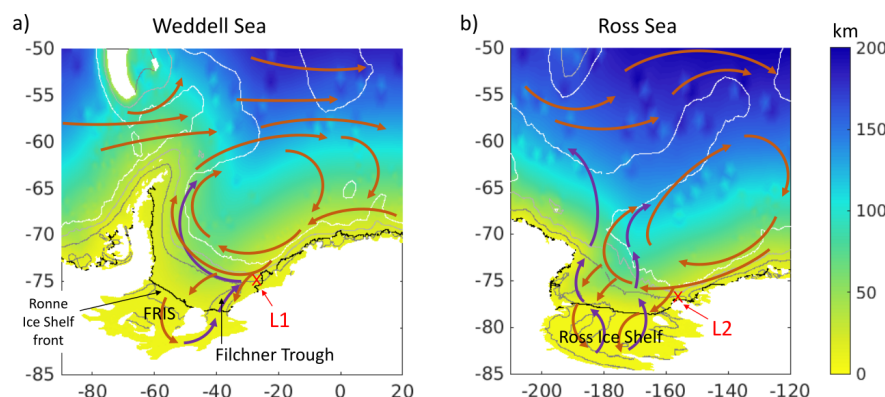
Figure 2. Detail views of the global model domain: a) Weddell Sea, b) Ross Sea. The grid resolution is shown in color, with ice shelf fronts (black line), 650-m isobath (dark grey), 2000-m isobath (light grey) and 3500-m isobath (white) added. Locations L1 and L2 are marked with a red cross. A simplified sketch of the circulation is overlaid with brown (warm) and purple (cold) water pathways.

50   warm regime shift on Antarctic continental shelves and its triggering mechanisms. In the following, we present the results of sensitivity studies with the global Finite Element Sea-ice Ocean Model (FESOM) aimed to (a) force a regime shift on the continental shelves of the Antarctic marginal seas using only manipulations of the atmospheric forcing and (b) identify the decisive factors that determine whether such a regime shift occurs.

2   Methods

55   ### 2.1   Model

The Finite Element Sea ice-Ocean Model (FESOM) version 1.4 is a primitive-equation hydrostatic ocean model that is solved on a horizontally unstructured mesh (Wang et al. 2014). It contains a dynamic-thermodynamic sea ice model (Danilov et al. 2015). The ice-shelf component (Timmermann et al., 2012) has been derived from the Hellmer and Olbers (1989) 3-equation model of ice shelf-ocean interaction with a velocity-dependent parameterization of boundary-layer heat and salt

60   fluxes according to Holland and Jenkins (1999). The model has been coupled to an ice sheet model (Timmermann and Goeller, 2017), but we use it with a constant ice-shelf geometry and bottom topography derived from RTopo-2 (Schaffer et al., 2016) to reflect the present-day state as realistically as possible.

We use FESOM in a global configuration with a horizontal resolution ranging from 4 km in the southern Weddell and Ross Seas, in the areas of the Antarctic coastline and ice shelves, to ≈120 km at the outer edge of the southern subpolar gyres

65   and increasing to 270 km in the vast mid-latitude ocean basins (Fig. 2). The vertical discretization uses 99 unevenly spaced z-levels, starting with 5-m layers at the surface. Temperature and salinity are initialized with the World Ocean Atlas (WOA) 2013 climatography (Locarnini et al., 2013; Zweng et al., 2013). The model is started from rest.

2.2 Forcing data sets

ERA Interim: A well-established re-analyis data set of the European Centre for Medium-Range Weather Forecasts (ECMWF)

70 (Dee et al., 2011). For the period 1979-2017, we use the 10-m zonal wind, 10-m meridional wind, 2-m air temperature, 2-m dew-point temperature, evaporation, precipitation, shortwave radiation, and longwave radiation. Of these, the first four have a temporal resolution of 6 hours, the latter four of 12 hours. The data set contains 365 days per year and accounts for leap years.

HadCM3: The atmospheric output of a fully coupled climate model of the Met Office Hadley Centre (Johns et al., 2011). The variables available to us are the 10-m zonal wind, 10-m meridional wind, 1.5-m air temperature, specific humidity, shortwave

75 radiation, and longwave radiation. The data set contains daily fields and uses a universal, idealized year with 360 days. HadCM3 20C represents a historic simulation for the 20th century (1900-1999), HadCM3 21C-A1B covers the 21st century (2000-2099) and is based on the SRES-A1B climate scenario. For our purposes, we calculated a dew point temperature T_d from the specific humidity H_s under consideration of the air temperature T_a. We used both the empirical relationship between relative humidity H_r and T_d

80 $$H_r = \frac{\epsilon_s(T_d)}{\epsilon_s(T_a)} = \frac{\epsilon_0 \, e^{5423 \, \mathrm{K} \left(\frac{1}{T_0} - \frac{1}{T_d} \right)}}{\epsilon_0 \, e^{5423 \, \mathrm{K} \left(\frac{1}{T_0} - \frac{1}{T_a} \right)}} \qquad (1)$$

with the saturation water vapour pressure ϵ_s, an empirical constant ϵ_0 of which the solution is independent, and the reference temperature $T_0 = 273.16$ K, and the relationship between H_r and H_s

$$H_r = \frac{0.263 \, p \, H_s}{e^{\left(\frac{17.67 \, (T_a - T_0)}{T_a - 29.65 \, \mathrm{K}} \right)}} \qquad (2)$$

with pressure p assumed to be 101.3 kPa.

2.3 Experiments

85

In the framework of the TiPACCs project, we conducted an extensive suite of experiments with different perturbations of the atmospheric forcing. Of these, the following nine runs featured in this publication will be referred to by the names:

REF: Forced by unaltered ERA Interim data, serving as reference run. The years 1979-2017 are repeated four times after a first cycle, which serves as spin-up period for this and all other experiments. Therefore, we count the spin-up as cycle 0 and

90 the following repeats as cycles 1 through 4.

To investigate causation of the regime shift:

SA_G: The seasonal cycle of the ERA Interim data was globally altered by adding a seasonal anomaly. This anomaly was calculated by subtracting the mean seasonal cycle of ERA Interim for the period 1980-1999 from the mean seasonal cycle of HadCM3 21C-A1B for the period 2070-2089, using a 30-day running mean. This period in the second half of the 21st century

95 was chosen because previous experiments (Timmermann and Hellmer, 2013) showed the interval to be prone to a regime shift on the Weddell Sea continental shelf. The anomaly varies with location and day-of-year. To make the data sets compatible, the specific humidity of the HadCM3 21C-A1B data was converted to the dew point temperature before determining the mean

seasonal cycle. In addition, every 60th day of the HadCM3 21C-A1B data was repeated to account for the difference in length of year. Short term and interannual variability of the ERA Interim data are thus maintained, while annual mean and shape of
100   the seasonal cycle are altered to resemble those of HadCM3 21C-A1B.

     SA_S: The same alterations to the forcing data were applied as described for SA_G, but only in the region south of 50°S. North of this line the ERA Interim forcing remains unaltered.

     SA_W: The same alterations to the forcing data were applied as described for SA_G, but only in the region of the Weddell Sea (south of 63°S and between 0° and 61°W). Outside of this area the ERA Interim forcing remains unaltered.

105   **SUMMER_S**: The duration of the austral summer season is prolonged by running every day of January three times while the austral winter months July and August are eliminated. The forcing is only applied south of 50°S. North of this line the ERA Interim forcing is unaltered.

     SUMMER_S_SAw_W: Same as SUMMER_S with the exception of the zonal and meridional wind components. For the Weddell Sea, to both wind components a seasonal anomaly is added that is abstracted from the anomaly used in SA_W by
110   using a fitted sine curve (with periodicity of one year) and spatial smoothing.

     To investigate reversal behaviour:

     R_ERA: A reversal run using unaltered ERA Interim data, same as the reference run REF. However it starts from a warm state FRIS cavity (branch-off after cycle 2 of SA_G).

     R_H20C: A reversal run using unaltered HadCM3 20C data. Like R_ERA, it starts from a warm-state FRIS cavity (branch-
115   off after cycle 2 of SA_G).

     H20C: A run using unaltered HadCM3 20C data (same as R_H20C), but starting from a cold-state FRIS cavity (branch-off after spin-up cycle 0 of REF).

3   Results

3.1   Warm inflow at FRIS

120 Several of our experiments using perturbations of the atmospheric forcing show a regime shift towards a sustained flow of Modified Warm Deep Water (MWDW) onto the continental shelf in the southern Weddell Sea. Of these, four will be discussed in detail in this publication.

     The first three of these experiments (SA_G, SA_S, and SA_W) – all applying a perturbation based on the HadCM3 21C-A1B seasonal anomaly, see section 2.3 – show a freshening and warming of the Weddell Sea continental shelf waters (Fig. 3a,b).
125 About 30-40 years after we started to apply the perturbation, FRIS melt rates rapidly increase up to 20 times compared to REF (Fig. 3c). During the same time interval, the Weddell Sea continental shelf appears to reach a new relatively stable state with a mean temperature increased, compared to REF, by 0.5 K in SA_W and approximately 1 K in SA_G and SA_S. Salinity is decreased by approximately 0.2 psu, 0.5 psu, and 0.4 psu, compared to REF, respectively. The coincidence of the abrupt change to higher basal melt rates and the end of the transient temperature increase on the continental shelf does not indicate
130 a causality. Temperature maps (Figure 5) show that the temperature has reached its maximum defined by the available heat in
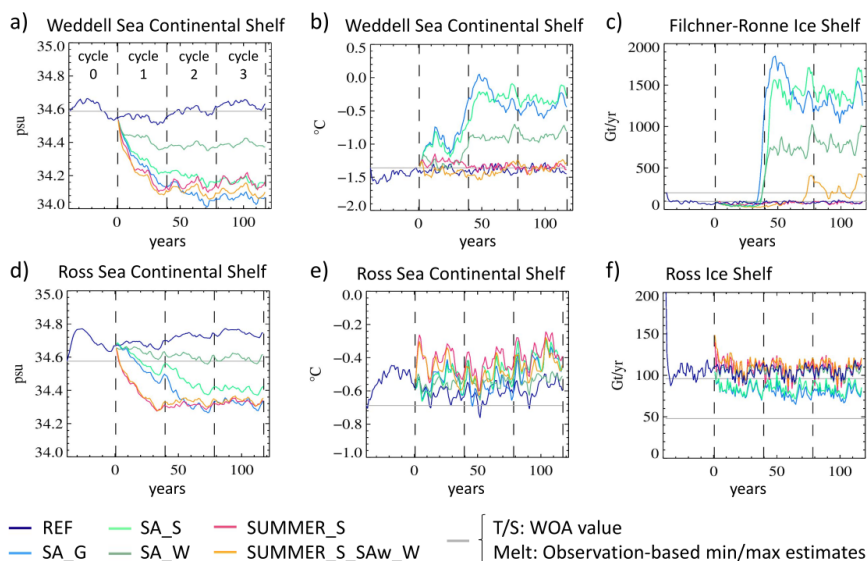
Figure 3. a) Annual mean salinity on the Weddell Sea continental shelf (averaged over volume below 200 m depth), b) annual mean temperature of the Weddell Sea continental shelf (averaged over volume below 200 m depth), and c) area-averaged annual mean FRIS melt rates, d-f) same for Ross Sea continental shelf and Ross Ice Shelf.

the WDW present at the continental shelf break. The data does not provide strong evidence of any feedbacks of the enhanced meltwater supply on the water mass characteristics.

Comparing the development of the continental shelf hydrography between the different SA_* experiments shows that the influence of forcing anomalies applied to the ocean north of the Antarctic Circumpolar Current (ACC) is comparatively small.
135 Global forcing manipulation triggers a stronger reduction in shelf salinities compared to the regional perturbations, and the initial response of shelf temperatures and melt rates in SA_G surpasses that of SA_S alongside with a slightly earlier jump in melt rates (exceeding 200 Gt/yr in year 35 vs. year 38). This initial maximum is, however, followed by a short decrease, and after year 62 both temperatures and melt rates remain below the values found in SA_S.

In SA_W, where a perturbation is applied only to the Weddell Sea, the response in both temperature and salinity, is about
140 half of what we see in SA_S, where a circumpolar perturbation is applied. The rapid melt rate increase in SA_W occurs at the same time as in SA_S, surpassing 200 Gt/yr in year 38. However, the meltrates yielded in the new steady state reflect the same factor ≈2 as found in the on-shelf temperatures and salinities.

The differences between these three experiments clearly underline the importance of the ACC and the influence of other Antarctic regions for the Weddell Sea. The regime shift on the continental shelf is by no means an event dependent on local
145 changes only, but is strongly influenced by far-field processes. The entire Southern Ocean is efficiently shielded from mid-latitude influence by the ACC. However, disruptions and anomalies are carried from one region of the Southern Ocean to the next by the ACC and, in the opposite direction, by the slope/coastal current with an impact on local water mass characteristics.
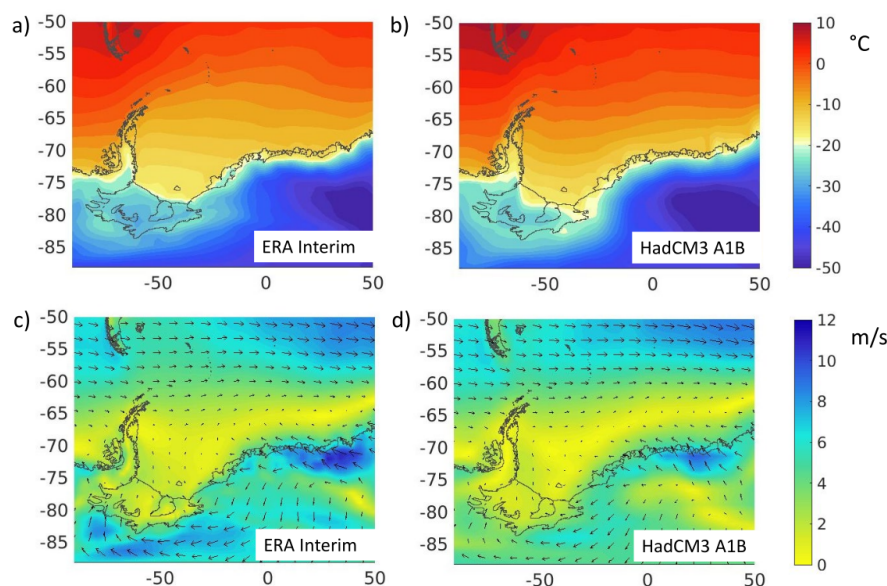
Figure 4. a) 20-year mean of air temperature from ERA Interim (1980 – 1999) and b) HadCM3 21C-A1B (2070 – 2089). c) 20-year mean wind field of ERA Interim (1980 – 1999) and d) HadCM3 21C-A1B (2070 – 2089). Speed is indicated by color, direction by the angle of the arrows at their point of origin.

Both air temperature and wind field exact a strong influence on the ocean. Over the ACC, the HadCM3 21C-A1B data features much higher air temperatures than ERA Interim and also the westerlies are stronger in this region (Fig. 4).

150   The experiments SUMMER_S and SUMMER_S_SAw_W, despite showing substantial freshening on the continental shelf, do not feature a prominent increase in mean shelf water temperature (Fig. 3a,b). While in SUMMER_S, we also find no substantial rise in FRIS basal melt rates, SUMMER_S_SAw_W features a late, comparatively low increase in FRIS basal melting ($\approx$ factor 3, Fig. 3c), triggered by a narrow inflow of mWDW into the Filchner Trough (Fig. 5f). These two experiments defy the expectation that a strong freshening of the continental shelf must necessarily lead to a strong warming, but also that

155 only a strong warming on the continental shelf can provoke a multiplication of the basal melt rate at the adjacent ice shelf. The two SUMMER_* experiments will be discussed in more detail in the following subsection.

     In the Ross Sea, all applied atmospheric perturbations also lead to a freshening and warming of the waters on the continental shelf (Fig. 3d–f). However, the temperature increase is generally limited to 0.2 K or less with already higher shelf temperatures in REF (-0.6°C compared to -1.3°C in the Weddell Sea). Similarly, salinity on the Ross Sea continental shelf hardly ever drops

160 below 34.3 psu, which caps the freshening at approximately 0.4 psu. In this context it should be noted that in our experiments the salinity on the Ross Sea shelf is rising during the spin-up cycle, which creates a positive saline bias of about 0.1 psu compared to the WOA data.

     In none of our experiments we find a substantial flow of warm water onto the Ross Sea continental shelf. Consequently, ice shelf basal melt rates show only small divergences from REF of the order of 10 Gt/yr in either direction depending on
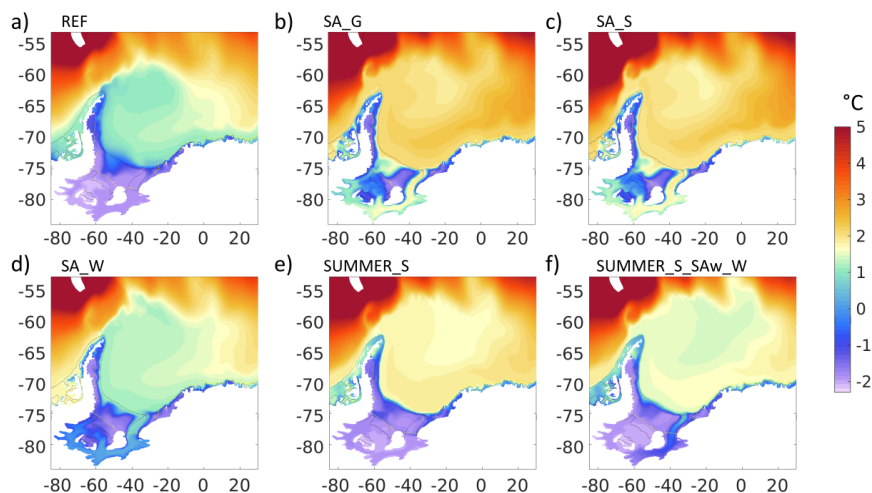
Figure 5. Temperature maximum in the water column of the Weddell Sea (mean of year 67 – 78) for experiments (a) REF, (b) SA_G, (c) SA_S, (d) SA_W, (e) SUMMER_S, and (f) SUMMER_S_SAw_W.

165   the experiment. We will, therefore, focus our analysis on the Weddell Sea and the fringing FRIS, and establish principles that might also apply to other marginal seas.

3.2 Deciding elements for warm water inflow

The experiment SUMMER_S is included in the suite of featured experiments because it demonstrates what keeps the continental shelf stable. At first glance, it seems to bring all necessary ingredients for a regime shift on the Weddell Sea continental
170   shelf: The on-shelf water experiences thorough freshening, there is evidence of warming on the shelf in cycle 1, and both of these changes exceed what is found for SA_W, where a regime shift is triggered.

Furthermore, like SA_G and SA_S, SUMMER_S exhibits a strong warming of the Weddell Gyre compared to REF (Fig. 5) along with an intensification of the gyre circulation (from an average of 29 Sv in year 30-39 in REF to 38 Sv, 36 Sv, and 39 Sv in SA_G, SA_S, and SUMMER_S, respectively). Along with a much warmer southern branch of the Weddell Gyre and
175   reduced sea ice cover goes a warm, surface-intensified western branch of the Weddell Gyre that follows the coastline at the tip of the Antarctic Peninsula into the Bellingshausen Sea. In all these characteristics, SUMMER_S is no different from runs featuring regime shifts, but the continental shelf and the ice shelf cavity in SUMMER_S remain protected from the off-shelf changes.

The crucial criterion for the warm water to cross the continental shelf and fill the ice shelf cavity is the balance between the
180   density off-shelf at sill depth and the densest water produced by sea ice formation on the continental shelf. In the Weddell Sea, the most active polynya exists in front of Ronne Ice Shelf (Haid and Timmermann, 2013) with a seasonal fluctuation of the location of the densest water either found on the eastern or the western side of the Ronne Ice Shelf front.

We therefore compare the maximum bottom density found along the Ronne Ice Shelf front as a measure of HSSW properties with the bottom density at the shelf break at a position east of (i.e. upstream from) the Filchner Trough sill at 670 m depth

185 (approximate sill depth, location L1 in Fig. 2) as a measure for the properties of the WDW at issue. As seen in Fig 6a, REF densities exhibit a slight positive trend with the HSSW in front of Ronne Ice shelf typically 0.3 kg m^{-3} denser than the WDW at the shelf break.

In the perturbation experiments SA_G and SA_S (Fig. 6b, c), the HSSW features a strong density loss in the first 4-5 decades as a reaction to the altered atmospheric forcing. Although also WDW density decreases in these experiments (by between 0.2

190 and 0.22 kg m^{-3}), at around year 30 it becomes the densest of the two water masses. A direct comparison between these two experiments shows that the WDW density loss is slightly diminished and slowed down by applying the forcing perturbation only to the southern part of the globe. With further restriction of the perturbation area in SA_W (Fig. 6d), the off-shelf density remains relatively stable. It exhibits a slight positive trend, but smaller than in REF.

For all members of the SA_* family of experiments, the maximum density found on the continental shelf off Ronne Ice

195 Shelf decreases by 0.3-0.6 kg m^{-3} (red lines in Fig. 6 b-d), since sea ice formation is strongly reduced by our perturbation of the atmospheric forcing. While SA_G is the experiment with the strongest off-shelf density loss, its on-shelf density decreases even more. Thus, in all cases, the on-shelf density decreases below the off-shelf density after between 30 and 40 years, allowing the warm off-shelf waters to replace the cold waters in the FRIS cavity.

In SUMMER_S (Fig 6e), the off-shelf density remains below the on-shelf density and although water mass characteristics

200 have changed on-shelf and off-shelf, the continental shelf remains protected by a persisting, albeit more vulnerable density contrast. It then only takes a change in the regional wind pattern (SUMMER_S_SAw_W) to further inhibit sea ice production and reduce the on-shelf density. The weaker northward winds in HadCM3 21C-A1B (Fig. 4) cause a more persistent sea ice cover in the southwestern Weddell Sea, and therefore a decrease of both on-shelf salinity (Fig 3a) and the maximum density in front of Ronne Ice Shelf (Fig 6f). In contrast to SUMMER_S, the SUMMER_S_SAw_W on-shelf density dips, at least

205 temporarily, below the off-shelf density, immediately triggering warm water flow onto the continental shelf and into the cavity via the Filchner Trough.

After year 70 in SUMMER_S_SAw_W, the maxima and minima seen in the FRIS basal mass loss (Fig. 3c) can be clearly associated with the extremes in the maximum density in front of Ronne Ice Shelf (Fig. 6f). In this case, the density balance is so sensitive that the mean basal melting of FRIS is controlled by sea ice production on the continental shelf. One should

210 note, however, that salinity – the governing control on density in the region – is a product not only of local processes but of the accumulated history of the water parcel (Haid et al., 2015). In the other experiments, once a warm state is established (year 40+), mean FRIS basal melting shows a clear dependence on the mean temperature on the continental shelf (cf Fig. 3b and c).

A similar analysis of on- and off-shelf densities for the Ross Ice Shelf (Fig. 7) reveals that the dense shelf water experiences a density loss of up to 0.5 kg m^{-3} in some of the experiments. However, the density of the Circumpolar Deep Water (CDW)

215 also features a reduction of up to 0.3 kg m^{-3} and thus remains lower in all cases. The smallest density difference occurs at
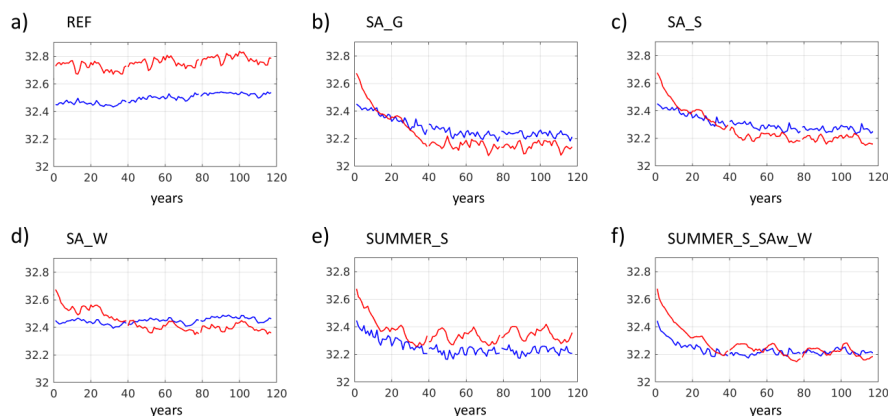
Figure 6. Annual mean values of maximum density σ_1 (potential density anomaly with reference pressure of 1000 dbar; reference density 1000 kg m^{-3}) along the Ronne Ice Shelf front (red) and bottom density at 670 m depth at the continental shelf break at location L1 marked in Fig. 2 (blue) for experiments (a) REF, (b) SA_G, (c) SA_S, (d) SA_W, (e) SUMMER_S, and (f) SUMMER_S_SAw_W. The depth of L1 is determined by the z-level closest to the Filchner Trough sill depth, which in the model is 640 m, slightly lower than in reality.
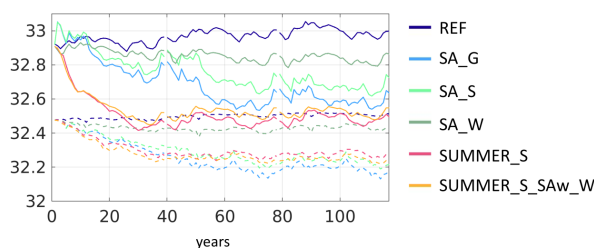
Figure 7. Annual mean values of maximum density σ_1 (potential density anomaly with reference pressure of 1000 dbar; reference density 1000 kg m^{-3}) along the Ross Ice Shelf front (solid) and bottom density (575-m depth) at the continental shelf break (dashed) at location L2 marked in Fig. 2 for the same experiments as shown in Fig. 6.

around year 30 in SUMMER_S, but even then the on-shelf density surpasses that of the CDW by 0.1 kg m^{-3}. This stability is favoured by the salinity bias found on the Ross Sea continental shelf in our model.

3.3 Reversibility and evidence of hysteresis behaviour

In order to fulfill the strict definition of a tipping point, the return from a tipped, warm ocean to the initial, cold state should not
220 be as easy as just reversing forcing conditions back over the tipping threshold, but requires an additional effort to shift them beyond a reversal threshold. For a tipping point, we expect hysteresis behaviour when switching from one state to the other compared to the reverse (see also Fig. 1).
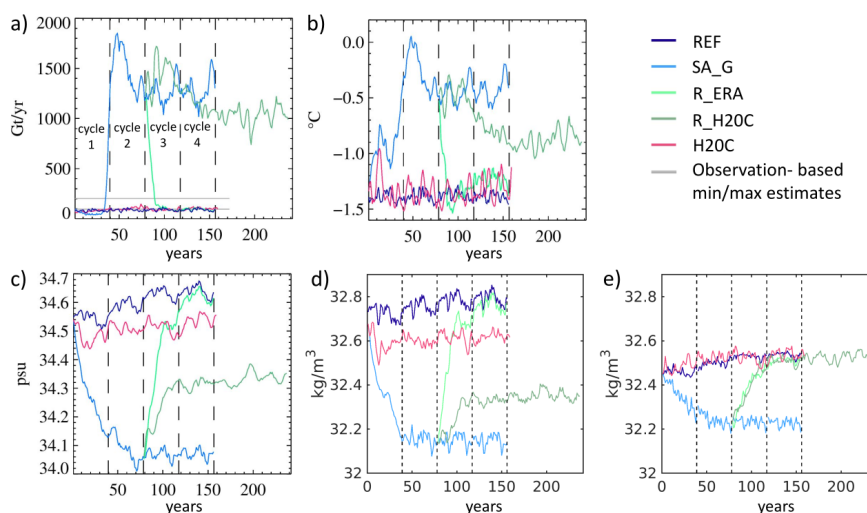
Figure 8. Area-averaged annual mean values of (a) FRIS basal mass loss, (b) temperature and (c) salinity on the Weddell Sea continental shelf (both below a depth of 200 m), (d) maximum density along the Ronne Ice Shelf front, and (e) bottom density near the Filchner Trough sill (Location L1) for the experiments listed in the upper right corner.

As a quick test for evidence of the regime shift on continental shelf actually being a tipping point, we branched off two reversal experiments, R_ERA and R_H20C after cycle 2 of SA_G (see Fig. 3). These experiments thus start with a warm
225 Weddell Sea continental shelf and show its evolution for current/last century atmospheric conditions.

The results show that an instantaneous return to unaltered ERA Interim forcing causes a rapid decrease of FRIS basal melt rates (light green line in Fig. 8a), which is linked to a rapid cooling (Fig. 8b) and salinity increase (Fig. 8c) on the continental shelf. As soon as the shelf waters off Ronne Ice Shelf (Fig. 8e) are denser than the waters off-shore at sill depth (Fig. 8d), they inevitably intrude into the cavity due to the southward sloping bathymetry. Depending on the volume of dense water produced
230 by sea ice formation, this will diminish or prevent the flow of warm water into the cavity.

Within two decades, a thermal state similar to the REF cold state is re-established on the southern Weddell Sea continental shelf (Fig. 8a,b). Basal melt rates and shelf temperatures are at the same level as in REF even though shelf salinity is still slightly fresher and it takes a few decades to return to its cold-state values (Fig. 8c). Again, the decisive factor is the density balance between the waters influenced by sea ice production on the continental shelf and the off-shelf waters of the Weddell
235 Gyre. The fast increase of the on-shelf water density (Fig. 8d) stops the inflow of WDW/MWDW into the cavity, which gets replaced with time by cold HSSW.

Using the 20th-century HadCM3 data to force the model starting from a warm state leads to a reduction of the melt rates (dark green lines in Fig. 8a). The inflow of warm water does not stop, since the density of the shelf water remains below the off-shelf water density. The existing density difference even facilitates a stronger inflow during the next 3 decades. In the long

240   term, however, basal melt rates decrease because of a cooling of WDW/MWDW by 2 K from 1.1 °C in SA_G (averaged over years 69-78) to -1.0 °C in R_H20C (years 108-117) at location L1 (Fig. 2).

With the same unaltered forcing (20th-century HadCM3 data), the model stays stable in a cold state if starting from a cold state (experiment H20C in Fig. 8). The forcing yields a higher long-term mean for the on-shelf temperatures and generally lower salinities than REF. Although the density difference is reduced compared to REF and it features a higher interannual

245   variability, the continental shelf remains stably in a cold state.

4   Discussion

We identified a density balance as the decisive factor for a regime shift on the southern Weddell Sea continental shelf. In order to penetrate onto the continental shelf and into the ice shelf cavities, the water at the shelf break at sill depth has to literally outweigh the water produced by sea ice formation on the continental shelf (with some inaccuracies due to mixing processes). In

250   a situation with moderate density gradients, this may lead to a protracted period of temporary and especially seasonal onshore flow, but any process causing the circumpolar waters to freshen less than the shelf waters will eventually tip the density balance in favour of the waters of open ocean origin. In consequence, the warmer off-shelf waters will replace the cold shelf waters in the cavity and enhance basal melting. We suppose that this continental shelf/shelf break process does exist not only in the Weddell Sea but in all other Antarctic marginal seas including the Ross Sea (as evidenced in Fig. 7) unless strong local

255   influences (e.g., winds, bottom topography) create an additional barrier at the continental shelf break.

It is no surprise that water density is crucial for a regime shift that allows WDW to penetrate onto the continental shelf and into fringing ice shelf cavities. Daae et al. (2020) found that a shoaling of the thermocline is important in triggering a warm inflow. In their regional model study, this was achieved by artificial manipulation of the boundary conditions that also entailed a lifting of the halocline and thus an increase in off-shelf water density at sill depth.

260   However, an increase of salinity at these depths is not a trend we observe around Antarctica (Schmidtko et al., 2014) or expect for the future. Instead, increased ice melt, - including sea ice, ice shelves, and icebergs - all around Antarctica causes a freshening of the Southern Ocean, especially in the coastal and slope currents (Strass et al., 2020). In accordance with these expectations for the future, we see freshening on- and off-shelf in all our experiments. The waters generally become warmer and fresher and therefore lighter. Only, if the on-shelf density falls below the density of the off-shelf waters at sill depth, the

265   latter will enter the continental shelf and fill up the deep parts of the ice shelf cavities. Our findings are also in accordance with the conceptual model proposed by Hazel and Stewart (2020), where the water mass density determines whether HSSW or WDW floods the ice shelf cavity.

The Weddell Sea continental shelf has a unique bathymetry which contributes to the vulnerability of its fringing ice shelves. The Filchner Trough with a sill depth of approximately 600 m allows deeper and denser off-shelf waters an easy access.

270   However, on-shelf salinity is a crucial factor when comparing the vulnerabilities of the Weddell and Ross Seas. During the spin-up cycle, our model experiences a slight freshening of the Weddell Sea and a salinity increase of the Ross Sea continental shelf. While the latter does indeed feature more saline water than the former, this difference is likely exaggerated in our model,

as evidenced by the bias in reference to the WOA data used for initialisation. Since the salinity dominates density on the continental shelves around Antarctica, this creates a much higher salinity threshold for the Ross Sea and keeps its continental shelf cold in all our experiments.

Even for FRIS, it turns out difficult to yield a regime change in the cavity by simple or idealized perturbations of the atmospheric forcing. As shortly mentioned in Section 2.3, in the framework of the TiPACCs project we conducted more than 70 experiments with different alterations of the atmospheric forcing. Of these, only a minority resulted in a change of the ocean to a warm-shelf state. The atmospheric forcing used in all these 'successful' experiments has some relationship to the HadCM3 21C-A1B output and involves changes in all or all-but-one forcing variables. All manipulations of a single or up-to-three atmospheric variables failed in inducing sustained warm water flow onto the continental shelf. Although air temperature and wind components were found to be important in the process, a manipulation of only these three variables in the same way as in SA_G was not sufficient to trigger the inflow. This lack of an 'easy recipe' within reasonable bounds reminds us that climate is a complex system with omnipresent non-linearities.

After the regime shift to a 'warm' state on the continental shelf, Hellmer et al. (2017) claim that the increased amount of melt water leads to a positive feedback on the cavity overturning circulation supporting a sustained inflow and an enhancement of basal melt rates. Therefore, a resistance of the system against a reversal is expected. However, the hysteresis behaviour, which is required for the strict definition of a tipping point, is not easy to demonstrate for a regime shift in an Antarctic ice shelf cavity. While Hazel and Stewart (2020) suceeded in mapping out a clear hysteresis curve for FRIS depending on meridional wind modifications (using a regional set-up and thus neglecting far-field influences on the Weddell Gyre), Caillet et al. (2022) could not find evidence of hysteresis investigating a possible past regime shift on the Amundsen Sea continental shelf.

Although the evolution of the water mass characteristics on the continental shelf gives no direct evidence toward the effect of a melt water feedback (Fig. 3), our experiments clearly show evidence of hysteresis behaviour: Depending on the starting state of the continental shelf, two different stable final states exist for the same forcing data set (HadCM3 20C). Based on our findings, we would locate the HadCM3 data for the 20th century, used in runs H20C and R_H20C, in the zone of bi-stability in a simplified scheme (Fig. 1), while placing the ERA Interim forcing to the left of the reversal threshold (both initial states yield the same final state). The forcing used for SA_G is located to the right of the tipping threshold (Fig. 1).

Our findings also underline that the range of bi-stability may not be very large and that with our still limited understanding of the complex system it can be difficult to find an atmospheric forcing data set that actually falls into this range. It may well be that current and/or last-century atmospheric conditions fall on the left side of the reversal threshold. Some caution is also advised: The climate system and its regional subsystems follow a complex interplay of a multitude of variables, which makes the 2D schematic a strong simplification of a multi-dimensional problem.

5 Conclusions

In our modelling study on the change of the ocean state on the Antarctic continental shelf, we identify the density balance between the off-shelf water at sill depth and the water produced by sea ice formation on the continental shelf as the decisive

factor determining whether the flow of off-shelf water into the deepest part of the continental shelf, i.e. the ice shelf cavities, is possible. Our experiments confirm the possibility for such a regime shift within the next 100 years for the FRIS cavity but not for the Ross Ice Shelf cavity. While the sill depth of the continental shelf certainly is one of the influential differences between the two regions, the higher salinity in the Ross Sea is more important since it keeps the density balance stable in all
310 our experiments.

We find that the ice shelf cavities may be better protected from the intrusion of warm WDW/CDW than previously expected (e.g., Hellmer et al., 2012). In a realistic future scenario not only the dense shelf waters linked to sea ice formation will undergo changes, but also the ACC, CDW/WDW characteristics, and the entire Southern Ocean will be affected by these changes. Both HSSW and WDW are expected to lose density but at different rates, since HSSW is primarily influenced by local atmospheric
315 events while the WDW/CDW characteristics depend more on the far-field. It is noteworthy, however, that a universal recipe for a regime shift in Antarctic marginal seas does not exist but that such a shift can occur under diverse circumstances and depends on local peculiarities ranging from bottom topography to atmospheric conditions.

Our results support the assumption that a cold-to-warm regime shift on the Weddell Sea continental shelf is a tipping point with hysteresis behaviour. The zone of bi-stability between the thresholds of tipping and reversal, however, may not be very
320 large. Potentially, present-day atmospheric conditions are on the 'cold' side of the bi-stability zone of the hysteresis.

Model studies with FESOM coupled to an ice sheet/ice shelf model (Timmermann and Goeller, 2017) show that enhanced basal melting of FRIS leads to an accelerated ice flow across the grounding line and thus contributes to global sea level rise. The model also demonstrates that the feedback of changing ice shelf geometry on cavity circulation does not cause qualitative differences in the relevant processes of ocean – ice shelf interaction. Compared to uncoupled simulations with constant present-
325 day cavity geometry, the coupled simulations yield a slightly stronger increase of basal melt rates in case of the ocean tipping into a warm state, but again results are not qualitatively different. We can therefore be confident that our results faithfully reflect the essential feedbacks between the different components of our model climate system.

By design, our study can only address regime shifts in the ocean (in the open ocean just as much as in sub-ice cavities); it cannot assess tipping points or instabilities in the cryosphere (e.g. accelerated ice mass flux through the speed-up of ice streams)
330 or coupled oceanic-cryospheric tipping points, like a marine ice sheet instability with irreversible grounding line retreat. In the framework of the TiPACCs project, several studies on ice shelf tipping points have already been conducted (Reese et al., 2022; Urruty et al., 2022) and coupled model studies are on the way.

Data availability. We will make our data available upon request.

Author contributions. VH conducted the numeric experiments, analysed and visualised the results and led the writing process; OG provided
335 the model geometry, read and commented on the manuscript; HHH conceived the idea for the study; RT and HHH contributed to the interpretation of results and to writing the manuscript.

Competing interests. None of the authors have any competing interests.

Acknowledgements. This work is part of the TiPACCs project, which receives funding from the European Union's Horizon 2020 research and innovation programme under grant agreement no. 820575. RT is supported by the Helmholtz Climate Initiative REKLIM (Regional Climate Change), a joint research project of the Helmholtz Association of German research centres (HGF). The work relied heavily on computational resources provided by the North German Supercomputing Alliance (HLRN).

340

References

Bull, C. Y. S., Jenkins, A., Jourdain, N. C., Vankova, I., Holland, P. R., Mathiot, P., Hausmann, U., and Sallee, J.-B.: Remote control of Filchner-Ronne Ice Shelf melt rates by the Antarctic Slope Current, J. Geophys. Res., 126, https://doi.org/10.1029/2020JC016550, 2021.

345 Caillet, J., Jourdain, N. C., Mathiot, P., Hellmer, H. H., and Mouginot, J.: Drivers and reversibility of abrupt ocean state transitions in the Amundsen Sea, Antarctica, Earth and Space Science Open Archive, p. 23, https://doi.org/10.1002/essoar.10511518.1, 2022.

Cornford, S. L., Martin, D. F., Payne, A. J., Ng, E. G., Le Brocq, A. M., Gladstone, R. M., Edwards, T. L., Shannon, S. R., Agosta, C., van den Broeke, M. R., Hellmer, H. H., Krinner, G., Ligtenberg, S. R. M., Timmermann, R., and Vaughan, D. G.: Century-scale simulations of the response of the West Antarctic Ice Sheet to a warming climate, The Croysphere, 9, 1579–1600, https://doi.org/10.5194/tc-9-1579-2015, 350   2015.

Daae, K., Hattermann, T., Darelius, E., Mueller, R. D., Naughten, K. A., Timmermann, R., and Hellmer, H. H.: Necessary conditions for warm inflow toward the Filchner Ice Shelf, Weddell Sea, Geophys. Res. Letters, 47, https://doi.org/10.1029/2020GL089237, 2020.

Darelius, E., Fer, I., and Nicholls, K. W.: Observed vulnerability of Filchner-Ronne Ice Shelf to wind-driven inflow of warm deep water, Nature Comm., 7:12300, https://doi.org/10.1038/ncomms12300, 2016.

355 Dee, D. P., Uppala, S. M., Simmons, A. J., Berrisford, P., Poli, P., Kobayashi, S., Andrae, U., Balmaseda, M. A., Balsamo, G., Bauer, P., Bechtold, P., Beljaars, A. C. M., van de Berg, L., Bidlot, J., Bormann, N., Delsol, C., Dragani, R., Fuentes, M., Geer, A. J., Haimberger, L., Healy, S. B., Hersbach., H, H. E. V., Isaksen, L., Kållberg, P., Köhler, M., Matricardi, M., McNally, A. P., Monge-Sanz, B. M., Morcrette, J.-J., Park, B.-K., Peubey, C., de Rosnay, P., Tavolato, C., Thépaut, J.-J., and Vitar, t. F.: The ERA-interim reanalysis: Configuration and performance of the data assimilation system, Q. J. R. Meteorol. Soc., 137, 553–597, https://doi.org/10.1002/qj.828, 2011.

360 Gladstone, R. M., Lee, V., Rougier, J., Payne, A. J., Hellmer, H. H., Le Brocq, A., Shepherd, A., Edwards, T. L., Gregory, J., and Cornford, S. L.: Calibrated prediction of Pine Island Glacier retreat during the 21st and 22nd centuries with a coupled flowline model, Earth Planet. Sci. Lett., 333–334, 191–199, https://doi.org/10.1016/j.epsl.2012.04.022, 2012.

Haid, V. and Timmermann, R.: Simulated heat flux and sea ice production at coastal polynyas in the southwestern Weddell Sea, J. Geophys. Res., 118, 2640–2652, https://doi.org/10.1002/jgrc.20133, 2013.

365 Haid, V., Timmermann, R., Ebner, L., and Heinemann, G.: Atmospheric forcing of coastal polynyas in the south-western Weddell Sea, Antarctic Science, 27, 388–402, https://doi.org/10.1017/S0954102014000893, 2015.

Hattermann, T., Nicholls, K. W., Hellmer, H. H., Davis, P. E. D., Janout, M. A., Østerhus, S., Schlosser, E., Rohardt, G., and Kanzow, T.: Observed interannual changes beneath Filchner-Ronne Ice Shelf linked to large-scale atmospheric circulation, Nature Comm., 12, https://doi.org/10.1038/s41467-021-23131-x, 2021.

370 Hazel, J. E. and Stewart, A. L.: Bistability of the Filchner-Ronne Ice Shelf cavity circulation and basal melt, J. Geophys. Res., 124, e2019JC015 848, https://doi.org/10.1029/2019JC015848, 2020.

Hellmer, H. H. and Olbers, D. J.: A two-dimensional model for the thermohaline circulation under an ice shelf, Antarctic Science, 1, 325–336, 1989.

Hellmer, H. H., Kauker, F., and Timmermann, R.: Weddell Sea anomalies: Excitation, propagation, and possible consequencs, Geophys. Res. 375   Letters, 36, L12 605, https://doi.org/10.1029/2009GL038407, 2009.

Hellmer, H. H., Kauker, F., Timmermann, R., Determann, J., and Rae, J.: Twenty-first-century warming of a large Antarctic ice-shelf cavity by a redirected coastal current, Nature, 485, 225–228, https://doi.org/10.1038/nature11064, 2012.

Hellmer, H. H., Kauker, F., Timmermann, R., and Hattermann, T.: The fate of the southern Weddell Sea continental shelf in a warming climate, jc, 30, 4337–4350, https://doi.org/10.1175/JCLI-D-16-0420.1, 2017.

380 Holland, D. M. and Jenkins, A.: Modeling thermodynamic ice-ocean interactions at the base of an ice shelf, J. Phys. Oceanogr., 29, 1787–1800, 1999.

Jenkins, A., Dutrieux, P., Jacobs, S., McPhail, S., Perrett, J., Webb, A., and White, D.: Observations beneath Pine Island Glacier in West Antarctica and implications for its retreat, Nature Geoscience, 3, 468–472, https://doi.org/10.1038/ngeo890, 2010.

Johns, T. C., Royer, J.-F., Höschel, I., Huebener, H., Roeckner, E., Manzini, E., May, W., Dufresne, J.-L., Otterå, O. H., Vuuren, D. P., Salas y
385 Melia, D., Giorgetta, M. A., Denvil, S., Yang, S., Fogli, P. G., Körper, J., Tjiputra, J. F., Stehfest, E., and Hewitt, C. D.: Climate change under aggressive mitigation: The ENSEMBLES multi-model experiment, Climate Dyn., 37, 1975–2003, https://doi.org/10.1007/s00382-011-1005-5, 2011.

Jourdain, N. C., Mathiot, P., Merino, N., Durand, G., Le Sommer, J., Spence, P., Dutrieux, P., and Madec, G.: Ocean circulation and sea-ice thinning induced by melting ice shelves in the Amundsen Sea, J. Geophys. Res., 122, 2550–2573, https://doi.org/10.1029/2003GL016941,
390 2017.

Klose, A. K., Karle, V., Winkelmann, R., and Donges, J. F.: Emergence of cascading dynamics in interacting tipping elements of ecology and climate, R. Soc. Open Sci., 7:200599, https://doi.org/10.1098/rsos.200599, 2020.

Lenton, T. M., Held, H., E., K., Hall, J. W., Lucht, W., Rahmstorf, S., and Schellnhuber, H. J.: Tipping elements in the Earth's climate system, Proc. Natl Acad. Sci. USA, 105, 1786–1793, https://doi.org/10.1073/pnas.0705414105, 2008.

395 Locarnini, R. A., Mishonov, A. V., Antonov, J. I., Boyer, T. P., Garcia, H. E., Baranova, O. K., Zweng, M. M., Paver, C. R., Reagan, J. R., Johnson, D. R., Hamilton, M., and Seidov, D.: World Ocean Atlas 2013, Volume 1: Temperature, in: NOAA Atlas NESDIS 73, edited by Levitus, S. and Mishonov, A., p. 40 pp, 2013.

Nakayama, Y., Schröder, M., and Hellmer, H. H.: From circumpolar deep water to the glacial meltwater plume on the eastern Amundsen Shelf, Deep-Sea Res., 77, 50–62, https://doi.org/10.1016/j.dsr.2013.04.001, 2013.

400 Naughten, K. A., Jenkins, A., Holland, P. R., Mugford, R. I., Nicholls, K. W., and Munday, D. R.: Modeling the Influence of the Weddell Polynya on the Filchner–Ronne Ice Shelf Cavity, J. Climate, 32, 5289–5303, https://doi.org/10.1175/JCLI-D-19-0203.1, 2019.

Naughten, K. A., De Rydt, J., Rosier, S. H. R., Jenkins, A., Holland, P. R., and Ridley, J. K.: Two-timescale response of a large Antarctic ice shelf to climate change, Nature Comm., 12:1991, https://doi.org/10.1038/s41467-021-22259-0, 2021.

Reese, R., Garbe, J., Hill, E. A., Urruty, B., Naughten, K. A., Gagliardini, O., Durand, G., Gillet-Chaulet, F., Chandler, D., Langebroek,
405 P. M., and Winkelmann, R.: The stability of present-day Antarctic grounding lines – Part B: Possible commitment of regional collapse under current climate, The Cryosphere Discussions, 2022, 1–33, https://doi.org/10.5194/tc-2022-105, 2022.

Ryan, S., Hellmer, H. H., Janout, M., Darelius, E., Vignes, L., and Schröder, M.: Exceptionally warm and prolonged flow of Warm Deep Water toward the Filchner-Ronne Ice Shelf in 2017, Geophys. Res. Letters, 47, e2020GL088 119, https://doi.org/10.1029/2020GL088119, 2020.

410 Schaffer, J., Timmermann, R., Arndt, J. E., Kristensen, S. S., Mayer, C., Morlighem, M., and Steinhage, D.: A global, high-resolution data set of ice sheet topography, cavity geometry, and ocean bathymetry, Earth System Science Data, 8, 543–557, https://doi.org/10.5194/essd-8-543-2016, 2016.

Schmidtko, S., Heywood, K. J., Thompson, A. F., and Aoki, S.: Multidecadal warming of Antarctic waters, Science, 346, 1227–1231, https://doi.org/10.1126/science.1256117, 2014.

415   Strass, V. H., Rohardt, G., Kanzow, T., Hoppema, M., and Boebel, O.: Multidecadal Warming and Density Loss in the Deep Weddell Sea,
           Antarctica, Journal of Climate, 33, 9863 – 9881, https://doi.org/10.1175/JCLI-D-20-0271.1, 2020.

       Thoma, M., Jenkins, A., Holland, D., and Jacobs, S. S.: Modelling Circumpolar Deep Water intrusions on the Amundsen Sea continental
           shelf, Antarctica, Geophys. Res. Letters, 35, 2008.

       Timmermann, R. and Goeller, S.: Response to Filchner-Ronne Ice Shelf cavity warming in a coupled ocean-ice sheet model - Part 1: The
420   ocean perspective, Ocean Science, 13, 765–776, https://doi.org/10.5194/os-13-765-2017, 2017.

       Timmermann, R. and Hellmer, H. H.: Southern Ocean warming and increased ice shelf basal melting in the twenty-first and twenty-second
           centuries based on coupled ice-ocean finite-element modelling, Ocean Dyn., 63, 1011–1026, https://doi.org/10.1007/s10236-013-0642-0,
           2013.

       Timmermann, R., Wang, Q., and Hellmer, H. H.: Ice shelf basal melting in a global finite-element sea ice/ice shelf/ocean model, Ann.
425   Glaciol., 53, https://doi.org/10.3189/2012AoG60A156, 2012.

       Urruty, B., Hill, E. A., Reese, R., Garbe, J., Gagliardini, O., Durand, G., Gillet-Chaulet, F., Gudmundsson, G. H., Winkelmann, R., Chekki,
           M., Chandler, D., and Langebroek, P. M.: The stability of present-day Antarctic grounding lines – Part A: No indication of marine ice
           sheet instability in the current geometry, The Cryosphere Discussions, 2022, 1–34, https://doi.org/10.5194/tc-2022-104, 2022.

       Zweng, M. M., Reagan, J. R., Antonov, J. I., Locarnini, R. A., Mishonov, A. V., Boyer, T. P., Garcia, H. E., Baranova, O. K., Johnson, D. R.,
430   Seidov, D., and Biddle, M. M.: World Ocean Atlas 2013, Volume 2: Salinity, in: NOAA Atlas NESDIS 74, edited by Levitus, S. and
           Mishonov, A., p. 39 pp, 2013.